Multicomponent Radial Flow Chromatography

T. Gu[1], G-J. Tsai[2], and G. T. Tsao[3]
[1] Department of Chemical Engineering, Ohio University, Athens, Ohio 45701, USA
[2] Building 130, Lederle Laboratories, Pearl River, NY 10965, USA
[3] Laboratory of Renewable Resources Engineering, 1295 Potter Center, Purdue University, West Lafayette, IN 479907-1295, USA

Radial flow chromatography (RFC) is an alternative to the conventional axial flow chromatography (AFC) in preparative and large scale applications. It provides a faster flow rate and a lower bed pressure drop. In this chapter a general nonlinear multicomponent rate model for RFC is presented. The radial dispersion and mass transfer coefficients are treated as variables in the model. The model was solved numerically by using finite element and orthogonal collocation methods for the discretizations of bulk-fluid and particle phase partial differential equations, respectively. Simulated examples are given for various chromatographic operations. The diffusional and mass transfer effects in RFC are studied. Some comparisons between AFC and RFC are shown. The model is also extended to include second order kinetics, size exclusion effect and reaction in the liquid phase for modeling of biospecific elution using soluble ligands.

Advances in Biochemical Engineering
Biotechnology, Vol. 49
Managing Editor: A. Fiechter

List of Symbols and Abbreviations

Symbol	*Description*
a_i	constant in Langmuir isotherm for component i, $b_i C_i^\infty$
b_i	adsorption equilibrium constant for component i, k_{ai}/k_{di}
Bi_i	Biot number of mass transfer for component i, $k_i R_p/(\varepsilon_p D_{pi})$
$\overline{Bi}_i$	averaged Bi_i
C_{bi}	bulk-fluid phase concentration of component i
C_{fi}	feed concentration profile of component i, a time dependent variable
C_{0i}	concentration used for nondimensionalization, $\max\{C_{fi}(t)\}$
C_{pi}	concentration of component i in the stagnant fluid phase inside particle macropores
C_{pi}^s	concentration of component i in the solid phase of particle (mole absorbate/unit volume of particle skeleton)
C_i^∞	adsorption saturation capacity for component i (mole adsorbate/unit volume of particle skeleton)
c_{bi}	$= C_{bi}/C_{0i}$
c_{pi}	$= C_{pi}/C_{0i}$
c_{pi}^s	$= C_{pi}^s/C_{0i}$
c_i^∞	$= C_i^\infty/C_{0i}$
D_{bi}	axial or radial dispersion coefficient of component i
$\bar{D}_{bi}$	averaged D_{bi}
D_{pi}	effective diffusivity of component i, porosity not included
h	axial bed length of the radial flow column
k_i	film mass transfer coefficient of component i
k_{ai}	adsorption rate constant for component i
k_{di}	desorption rate constant for component i
N	number of interior collocation points
Ne	number of quadratic elements
Ns	number of components
Pe_i	Peclet number of radial dispersion for component i, $\dfrac{v(X_1 - X_0)}{D_{bi}}$
Q	volumetric flow rate of the mobile phase
R	radial coordinate for particle
R_p	particle radius
r	$= R/R_p$
t	time
v	interstitial velocity
V_b	bed volume for RFC column, $\pi h(X_1^2 - X_0^2)$
V_0	dimensionless constant, $\dfrac{\pi h X_0^2}{V_b}$ or $\dfrac{X_0^2}{X_1^2 - X_0^2}$

V dimensionless volumetric coordinate, $\dfrac{\pi h(X^2 - X_0^2)}{V_b}$

or $\dfrac{X^2 - X_0^2}{X_1^2 - X_0^2} \in [0, 1]$

X radial coordinate for RFC column
X_1 outer radius of RFC column
X_0 inner radius of RFC column

Greek Letters

α $= 2\sqrt{V + V_0}(\sqrt{1 + V_0} - \sqrt{V_0})$
ε_b bed void volume fraction
ε_p particle porosity
η_i dimensionless constant, $\dfrac{\varepsilon_p D_{pi}}{R_p^2} \dfrac{V_b \varepsilon_b}{Q}$

ξ_i dimensionless constant for component i, $3Bi_i \eta_i (1 - \varepsilon_b)/\varepsilon_b$

τ dimensionless time, $\dfrac{Qt}{V_b \varepsilon_b}$

τ_{imp} dimensionless time duration for a rectangular pulse of a sample
ϕ Lagrangian interpolation function

1 Introduction

Chromatography has long been established as an effective means of separation. It is becoming more and more popular in the age of the rapid development of biotechnology. The demand for efficient preparative and large scale liquid chromatographic separation processes is steadily increasing. Radial flow chromatography (RFC), since its introduction onto the commercial market in the mid 1980s [1], has proved to be a promising alternative to conventional axial flow chromatography (AFC). Compared to AFC, the RFC geometry (Fig. 1) provides a relatively large flow area and short flow path. These factors enable a larger volumetric flow rate and shorter shift time in liquid chromatographic separations. Its soft gels or affinity matrix materials are used as separation media, the low pressure drop of RFC helps prevent bed compression [2, 3]. A full range of sizes from 50 ml to 200 l in bed volume of RFC columns both prepacked and unpacked can be obtained from commercial companies. Separation of various biological products has been reported [2, 4, 5, 6, 7, 8, 9]. An experimental case study of the comparison of RFC and AFC was carried out by Saxena and Weil [5] for the separation of ascites using QAE cellulose packings. They reported that by using a higher flow rate, the separation time for RFC was one-fourth that needed for a longer AFC column with the same bed volume. It was claimed that by using RFC instead of AFC, separation productivity can be improved quite significantly [1]. RFC is especially suitable for affinity chromatography in which solutes are usually strongly retained. This permits the use of a high flow

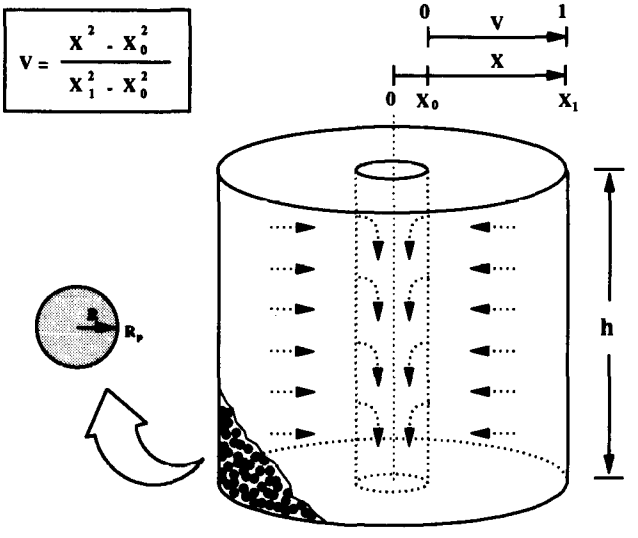

Fig. 1. Structure of a cylindrical radial flow column

rate and a short flow path for the fast treatment of a large volume of samples. RFC is advantageous for separation processes in which the effluent from the column is being recycled and the adsorbate will not be lost in the effluent stream [10], such as in the case of in situ separation (integrated process) [11].

Radial flow packed-bed reactors have been used for a variety of industrial applications such as ammonia and methanol syntheses, catalytic reforming, and vapor-phase desulfurization [12, 13]. Unlike the radial flow reactor, RFC is used primarily for liquid phase chromatographic separations. There are quite a few papers that are related to the theoretical and experimental studies of radial flow reactors. A brief review was given by Hlavacek and Votruba [14]. More recent papers include Strauss and Budde [13], Balakotaiah and Luss [12], Chang et al. [15], Lepez de Ramos and Pironti [16], and Tharakan and Chau [17]. The study of RFC may provide some useful information for the understanding of mass transfer processes in radial flow reactors.

Because of the special flow geometry in RFC some complications may arise in mathematical modeling. Since the linear flow velocity (v) in the RFC column changes constantly along the radial coordinate of the column (Fig. 1), unlike in most cases of AFC, the radial dispersion and external mass transfer coefficients are no longer constants. This important feature was rarely considered in the mathematical modeling of RFC in the literature in the past. Extensive theoretical studies have been reported for single component ideal RFC, which neglects radial dispersion, intraparticle diffusion, and external mass transfer resistance. In such studies a local equilibrium and a linear isotherm were often assumed. The earliest theoretical treatment of RFC was done by Lapidus and Amundson [18]. A similar study was carried out by Rachinskii [19]. Later Inchin and Rachinskii [20] included bulk-fluid phase molecular diffusion in their model. Lee et al. [21], proposed a unified approach for moments in linear chromatography, both AFC and RFC. They used several single component rate models for the comparison of statistical moments for RFC and AFC. Their models included radial dispersion, intraparticle diffusion, and external mass transfer effects. Kalinichev and Zolotarev [22] also carried out an analytical study on moments for single component RFC in which they treated the radial dispersion coefficient as a variable.

A rate model for nonlinear single component RFC was solved numerically by Lee [23] by using the finite difference and orthogonal collocation methods. His model considered radial dispersion, intraparticle diffusion, external mass transfer, and nonlinear isotherms. It used averaged radial dispersion and mass transfer coefficients instead of treating them as variables. A nonlinear model of this kind of complexity has no analytical solution and must be solved numerically.

Rhee et al. [24], discussed the extension of their multicomponent chromatography theory for ideal AFC with Langmuir isotherms, which is a parallel treatise to the interference theory developed by Helfferich [25], to RFC. Apart from this, so far no other detailed theoretical treatment of nonlinear multicomponent RFC is available in the literature. With the development of powerful

computers and efficient numerical methods, more complicated treatment of multicomponent RFC now becomes possible. A general model for multicomponent RFC can provide some very valuable information.

In this chapter a numerical procedure is presented for solution to a general rate model for multicomponent RFC. The model is solved numerically. The solution of the model enables the discussion of several important issues concerning the characteristics and performance of RFC and its differences from AFC. And also the question of whether one should treat dispersion and mass transfer coefficients as variables in RFC.

2 General Multicomponent Rate Model for RFC

Consider a fixed bed with cylindrical radial flow geometry (Fig. 1) which is filled with uniform spherical porous solid adsorbents. Suppose the process is isothermal and there is no concentration gradient in the axial direction of the column. Although it can be a problem in some real cases, the possible maldistribution of flow streams is ignored in this theoretical study. Also, local equilibrium is assumed for each component between the pore surface and the liquid phase in the macropores in particles. Based on these basic assumptions, the following governing equations for component i in the bulk-fluid and particle phases via mass balances in the two phases can be formulated.

$$\frac{1}{X}\frac{\partial}{\partial X}\left(D_{bi}X\frac{\partial C_{bi}}{\partial X}\right) \pm v\frac{\partial C_{bi}}{\partial X} - \frac{\partial C_{bi}}{\partial t} + \frac{3k_i(1-\varepsilon_b)}{\varepsilon_b R_p}(C_{bi} - C_{pi,R=R_p}) = 0 \tag{1}$$

$$\frac{\partial}{\partial t}[(1-\varepsilon_p)C^s_{pi} + \varepsilon_p C_{pi}] - \varepsilon_p D_{pi}\left[\frac{1}{R^2}\frac{\partial}{\partial R}\left(R^2\frac{\partial C_{pi}}{\partial R}\right)\right] = 0 \tag{2}$$

where in Eq. (1) $+ v$ is for outward flow and $- v$ for inward flow. Note that in Eq. (1) D_{bi} and k_i are variables which are dependent on v.

The initial and boundary conditions are

$$t = 0, C_{bi} - C_{bi}(0, X) \quad C_{pi} = C_{pi}(0, R, X) \tag{3, 4}$$

$$R = 0, \frac{\partial C_{pi}}{\partial R} = 0 \quad R = R_p, \frac{\partial C_{pi}}{\partial R} = \frac{k_i}{\varepsilon_p D_{pi}}(C_{bi} - C_{pi,R=R_p}) \tag{5, 6}$$

For outward flow

$$X = X_0, \frac{\partial C_{bi}}{\partial X} = \frac{v}{D_{bi}}(C_{bi} - C_{fi}(t)) \quad X = X_1, \frac{\partial C_{bi}}{\partial X} = 0 \tag{7a, 8a}$$

and for inward flow

$$X = X_1, \frac{\partial C_{bi}}{\partial X} = \frac{v}{D_{bi}}(C_{bi} - C_{fi}(t)) \quad X = X_0, \frac{\partial C_{bi}}{\partial X} = 0 \tag{7b, 8b}$$

These equations can be expressed in the following dimensionless forms,

$$-\frac{\partial}{\partial V}\left(\frac{\alpha}{Pe_i}\frac{\partial c_{bi}}{\partial V}\right) \pm \frac{\partial c_{bi}}{\partial V} + \frac{\partial c_{bi}}{\partial \tau} + \xi_i(c_{bi} - c_{pi,r=1}) = 0 \tag{9}$$

$$\frac{\partial}{\partial \tau}[(1 - \varepsilon_p)c_{pi}^s + \varepsilon_p c_{pi}] - \eta_i\left[\frac{1}{r^2}\frac{\partial}{\partial r}\left(r^2\frac{\partial c_{pi}}{\partial r}\right)\right] = 0 \tag{10}$$

where for bulk-fluid phase equation (Eq. (9)) the local volume averaging method of Lee [23] and Slattery [26] has been used for its nondimensionalization. A comparison of the definitions of the dimensionless variables and parameters used in AFC and RFC is listed in Table 1.

In Eq. (9), the radial flow Peclet number is defined as $Pe_i = v(X_1 - X_0)/D_{bi}$. The introduction of the radial flow Peclet number and the use of the local volume averaging method in the transformation, streamline the analogy and

Table 1. Comparison of dimensionless variables and parameters

Symbols	AFC	RFC
τ	$\frac{t}{\left(\frac{L}{v}\right)}$	$\frac{t}{\left(\frac{V_b\varepsilon_b}{Q}\right)}$
z, V	$z = \frac{Z}{L}$	$V = \frac{X^2 - X_0^2}{X_1^2 - X_0^2}$
r	$\frac{R}{R_p}$	Same
Pe	$Pe_{Li} = \frac{vL}{D_{bi}}$	$Pe_i = \frac{v(X_1 - X_0)}{D_{bi}}$
Bi_i	$\frac{k_i R_p}{\varepsilon_{pi}^a D_{pi}}$	Same
η_i	$\frac{\varepsilon_{pi}^a D_{pi}}{R_p^2}\frac{L}{v}$	$\frac{\varepsilon_{pi}^a D_{pi}}{R_p^2}\frac{V_b\varepsilon_b}{Q}$
ξ_i	$\frac{3Bi_i\eta_i(1 - \varepsilon_b)}{\varepsilon_b}$	Same
V_0	—	$\frac{X_0^2}{X_1^2 - X_0^2}$
α	—	$2\sqrt{V + V_0}(\sqrt{1 + V_0} - \sqrt{V_0})$

comparison between the RFC model and the AFC model [27]. One may find that the dimensionless RFC rate model looks very similar to the dimensionless AFC rate model shown in an article by the same authors [28], except that in the RFC model there is an extra variable α and ξ is not a constant. Also, in RFC, there are two different flow directions, which are reflected by the $\pm$ sign in Eq. (9).

Initial conditions:

$$\tau = 0, \quad c_{bi} = c_{bi}(0, V), \quad c_{pi} = c_{pi}(0, r, V) \tag{11, 12}$$

Boundary conditions for outward flow:

$$V = 0, \frac{\partial c_{bi}}{\partial V} = \frac{Pe_i}{\alpha}\left[c_{bi} - \frac{C_{fi}(\tau)}{C_{0i}}\right] \tag{13}$$

For frontal adsorption, $C_{fi}(\tau)/C_{0i} = 1$

For elution, $C_{fi}(\tau)/C_{0i} = \begin{cases} 1 & 0 \le \tau \le \tau_{imp} \\ 0 & \text{else} \end{cases}$

After the sample has been introduced:

(in the form of frontal adsorption)

if component i is displaced, $\dfrac{C_{fi}(\tau)}{C_{0i}} = 0$

if component i is a displacer, $\dfrac{C_{fi}(\tau)}{C_{0i}} = 1$

$$V = 1, \quad \frac{\partial c_{bi}}{\partial V} = 0 \tag{14}$$

$$r = 0, \quad \frac{\partial c_{pi}}{\partial r} = 0 \quad r = 1, \frac{\partial c_{pi}}{\partial r} = Bi_i(c_{bi} - c_{pi,r=1}) \tag{15, 16}$$

For inward flow one only needs to swap $V = 0$ in Eq. (13) with $V = 1$ in Eq. (14).

The general solution strategy for the coupled partial differential equation (PDE) system (Eqs. (9) and (10)) is the same as that for the case of AFC discussed in the article by the same authors [28]. Compared to AFC, the solution for RFC seems to be more complicated because of variations in some physical properties of the system as mentioned earlier. The finite element method is apparently an ideal approach for this kind of system.

3 Numerical Solution

Equations (9) and (10) are transformed to a set of ODEs by the finite element method and the orthogonal collocation (OC) method [29], respectively.

Using the Galerkin approximation [30], Eq. (9) becomes

$$[DB_i][c'_{bi}] + [AKB_i][c_{bi}] = [PB_i] + [AFB_{bi}] \tag{17}$$

where $$(DB_i)^e_{m,n} = \int \phi_m \phi_n \, dV \tag{18}$$

$$(AKB_i)^e_{m,n} = \int \left(\frac{\alpha}{Pe_i} \frac{\partial \phi_m}{\partial V} \frac{\partial \phi_n}{\partial V} \pm \phi_m \frac{\partial \phi_n}{\partial V} + \xi_i \phi_m \phi_n \right) dV \tag{19}$$

$$(AFB_i)^e_m = \int \xi_i \phi_m c_{pi,r=1} \, dV \tag{20}$$

in which m, n = 1, 2, 3, and the superscript e indicates that the finite element matrices and vectors are evaluated over each individual element before global assembly. In Eq. (19), $+\phi_m$ is for outward flow and $-\phi_m$ for inward flow. The natural boundary condition $(PB_i) = -c_{bi} + C_{fi}(\tau)/C_{0i}$ is applied to $[AKB_i]$ and $[AFB_i]$ at V = 0 for outward flow or $(PB_i) = c_{bi} - C_{fi}(\tau)/C_{0i}$ at V = 1 for inward flow. $(PB_i) = 0$ elsewhere. Note that in Eq. (19) α is a function of V.

The particle phase equation can be discretized with N interior collocation points. The ODE system resulting from the numerical discretization can then be solved by Gear's stiff method. The procedure is the same as that for AFC which has been shown in the article by the same authors [28].

In this numerical procedure D_{bi} and k_i values are treated as variables which are dependent on the variations of v along the radial coordinate V. Meanwhile intraparticle diffusivities (D_{pi}) are regarded as independent of the variations of v. For dispersion coefficient, $D_b \propto v$ [23, 31]. This also applies to RFC. Thus the Pe_i can be treated as constants that are independent of v. It has also been shown [9] that

$$k_i \propto v^{1/3} \tag{21}$$

Since $k_i \propto v^{1/3}$ and

$$v \propto \frac{1}{X} \propto \frac{1}{\sqrt{V + V_0}} \tag{22}$$

one has

$$Bi_i \propto k_i \propto (1/X)^{1/3} \propto (V + V_0)^{-1/6} \tag{23}$$

If $Bi_{i,V=1}$ (i.e., $Bi_{i,X=X_1}$) values are given as input values, then

$$Bi_{i,V} = \left[\frac{1 + V_0}{V + V_0} \right]^{1/6} Bi_{i,V=1} \tag{24}$$

For ξ_i at any V position one has

$$\xi_{i,V} = \frac{3\eta_i(1 - \varepsilon_b) Bi_{i,V}}{\varepsilon_b} = \frac{3\eta_i(1 - \varepsilon_b)}{\varepsilon_b} \left[\frac{1 + V_0}{V + V_0} \right]^{1/6} Bi_{i,V=1} \tag{25}$$

Equation (25) is used for the evaluation of Eq. (19). In Eq. (19), due to the special geometry of radial flow chromatography, there are two space coordinates (V)

dependent variables, α and ξ_i. The finite element integral in Eq. (19) is evaluated for each local element and α, ξ_i can be dealt with routinely without any trouble, since in this chapter finite element integrals are evaluated using four point Gauss-Legendre quadratures [29]. The ability to deal with variable physical properties with ease is one of the well-known advantages of the finite element method. Accuracy is another notable advantage of the method. The accommodation of variable Bi_i in Eq. (22) for the particle phase is also very easy. Since particle phase equations must be solved at each finite element node (with given nodal position, V) in the function subroutine, $Bi_{i,V}$ values can be readily obtained from Eq. (24).

It is very helpful to study the effects of treating D_{bi} and k_i as variables compared to treating them as constants, as is the case in most of the existing papers in the literature. There are two easy ways to take averaged D_{bi} and k_i values for the modeling. In both cases $Pe_i = v(X_1 - X_0)/D_{bi}$ will no longer be constant. In all the RFC cases in this chapter in the input data for simulation $Bi_{i,V=1}$ values are given.

The discussion below shows how to modify the algorithm to accommodate cases using the averaged D_{bi} and k_i values in order to make comparisons.

Using v value at $V = 0.5$ for averaging D_{bi} and k_i

$$\frac{\alpha}{\overline{Pe_i}} = \frac{\alpha}{\dfrac{v(X_1 - X_0)}{\bar{D}_{bi}}} = \frac{\alpha}{\dfrac{v(X_1 - X_0)}{D_{bi}}\dfrac{D_{bi}}{\bar{D}_{bi}}} = \frac{\alpha}{Pe_i}\frac{\bar{D}_{bi}}{D_{bi}} \tag{26}$$

Since $D_{bi} \propto v$, from Eq. (22) it is easy to obtain

$$\frac{\alpha}{\overline{Pe_i}} = \frac{\alpha}{Pe_i}\sqrt{\frac{V + V_0}{0.5 + V_0}} \tag{27}$$

Eq. (24) gives

$$\overline{Bi_i} = Bi_{i,V=0.5} = \left[\frac{1 + V_0}{0.5 + V_0}\right]^{1/6} Bi_{i,V=1} \tag{28}$$

Using v value at $X = (X_1 + X_0)/2$ for averaging D_{bi} and k_i

$$\frac{\alpha}{\overline{Pe_i}} = \frac{\alpha}{Pe_i}\frac{\bar{D}_{bi}}{D_{bi}} = \frac{\alpha}{Pe_i}\frac{X}{(X_1 + X_0)/2} = \frac{\alpha}{Pe_i}\frac{\sqrt{V + V_0}}{(\sqrt{1 + V_0} + \sqrt{V_0})/2} \tag{29}$$

For Bi_i one has

$$\frac{Bi_{i(X_1+X_0)/2}}{Bi_{i,X_1}} = \left[\frac{X_1}{(X_1 + X_0)/2}\right]^{1/3} = \left[\frac{\sqrt{1 + V_0}}{(\sqrt{1 + V_0} + \sqrt{V_0})/2}\right]^{1/3} \tag{30}$$

which gives

$$\overline{Bi_i} = Bi_{i,(X_1+X_0)/2} = \left[\frac{\sqrt{1 + V_0}}{(\sqrt{1 + V_0} + \sqrt{V_0})/2}\right]^{1/3} Bi_{i,V=1} \tag{31}$$

If using averaged values of D_{bi} and k_i instead of treating them as v dependent variables, one needs to use $\alpha/\overline{Pe_i}$ in Eq. (27) or Eq. (29) to replace α/Pe_i in Eq. (19), and use $\overline{Bi_i}$ to replace Bi_i in Eq. (23). Bi_i should also be used to calculate ξ_i.

4 Results and Discussion

The multicomponent Langmuir isotherm and the stoichiometric isotherm are used for the simulations. Parameter values used in simulations are listed in Table 2, or mentioned during discussions.

4.1 Simulations of Different Chromatographic Operations

Figure 2 shows the simulated breakthrough curves for two components in inward and outward flow RFC. The corresponding breakthrough curves in AFC are also shown for comparison. They were obtained by using the same dimensionless parameters and isotherms as in the RFC case, except that $Bi_1 = Bi_2 = 11.15$ were used. These two Bi values for AFC are the ones its corresponding RFC possesses at V = 0.5. Figure 2 clearly shows that in RFC, inward flow provides sharper concentration profiles than outward flow. This is in agreement with the results obtained by Lee [23] for single component RFC. For a comparison similar to that shown in Fig. 2, the simulated effluent history

Table 2. Parameter values used for simulation*

		Physical parameters					Numerical parameters	
Figures	Species	Pe_{Li}	η_i	Bi_i	a_i	$b_i \times C_{0i}$	Ne	N
2	1	30	8	10	4	5×0.2	8	2
	2	30	8	10	8	10×0.2		
3	1	25	10	3	4	5×0.1	8	2
	2	25	10	3	8	10×0.2		
4	1	50	15	12	1	2×0.2	6	2
	2	65	20	8	10	20×0.2		
	1	90	10	40				
5	2	90	10	40			5	2
	3	90	10	40				
6	1	30	10	20	5	5×0.2	8	2
	2	30	10	20	6	6×0.8		

* In all runs, $\varepsilon_p = \varepsilon_b = 0.4$, and $V_0 = 0.04$ or otherwise as specified. For elution cases, sample size is $\tau_{imp} = 0.2$. For Fig. 5, $\alpha_{13} = 0.6$, $\alpha_{23} = 3$, $C_{01} = C_{02} = 0.1$, $C_{03} = 0.04$ N and $\bar{C} = 1.8\,\text{meq ml}^{-1}$ bed. The ODE solver's (IMSL's IVPAG subroutine) tolerance is tol = 10^{-5}. Double precision is used in the Fortran code. CPU times on SUN 4/280 computer for some simulations are: Fig. 2 (solid lines), 4.7 min; Fig. 3 (solid lines), 0.9 min; Fig. 4 (solid lines), 4.5 min

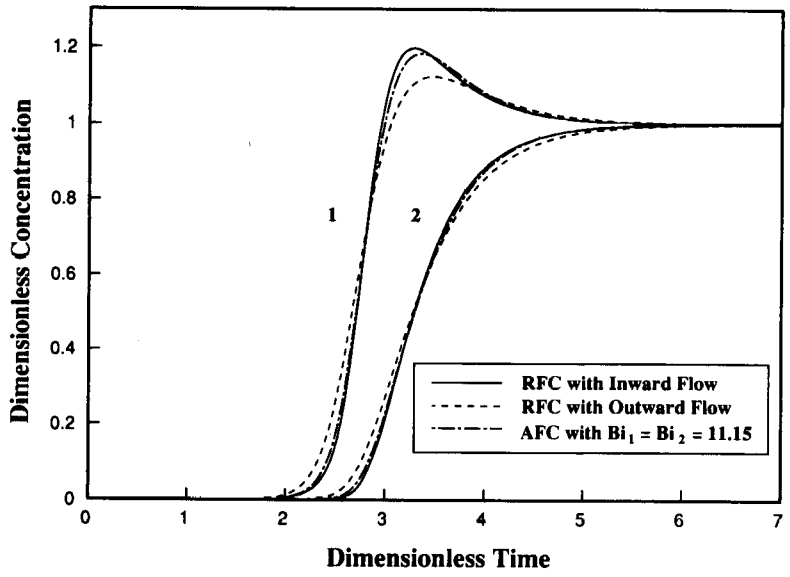

Fig. 2. Comparison of inward and outward flow RFC and AFC in frontal adsorption

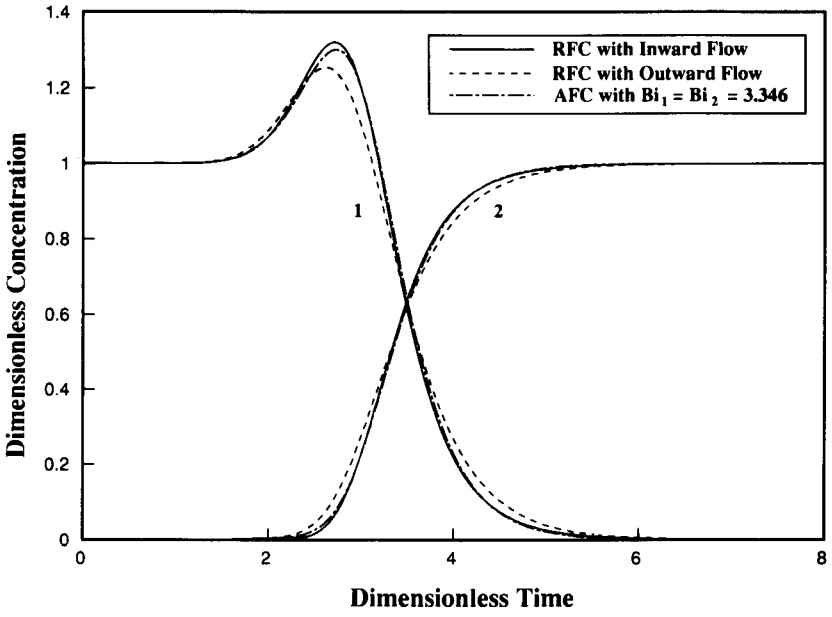

Fig. 3. Comparison of inward and outward flow RFC and AFC in displacement

for a step change displacement process is presented in Fig. 3. In this case the column is presaturated with component 1. Component 2 is introduced via a step change as a displacer to displace the adsorbed molecules of component 1. Again, inward flow RFC offers sharper concentration profiles, which are favorable for separation. The same conclusion also holds for the two component elution case shown in Fig. 4.

Figure 5 shows the chromatogram for isocratic elution of a binary sample (component 1 and component 2) with a small ion (component 3) as the eluent (component 3) in inward flow RFC. The separation factors are constants in this case ($\alpha_{13} = 0.6$, $\alpha_{23} = 3.0$). This is similar to the binary elutions with a competing modifier in the mobile phase.

Multi-stage operations can also be simulated with our code. Figure 6 shows the effluent history of a reverse flow displacement process, in which the displacer (component 2) is introduced with a reversed flow direction after an incomplete period of frontal adsorption of component 1, which lasted $\tau = 3$. Such reverse flow displacement operation is actually very common in industrial AFC practice [32] aimed at improving process efficiency and reducing column clogging. It has been used in the elution stage of affinity chromatography by Chase [33]. In Fig. 6, the combination of outward flow adsorption and inward flow displacement gives better results, since its process time is slightly shorter.

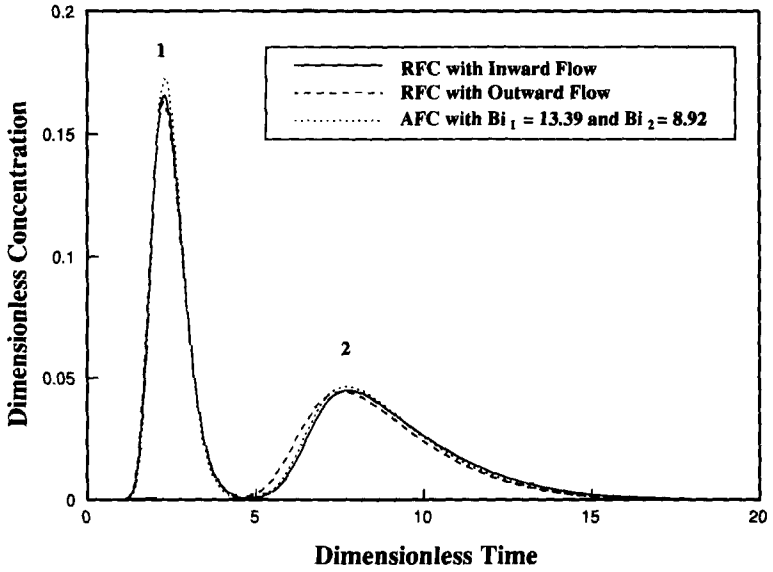

Fig. 4. Comparison of inward and outward flow RFC and AFC in elution

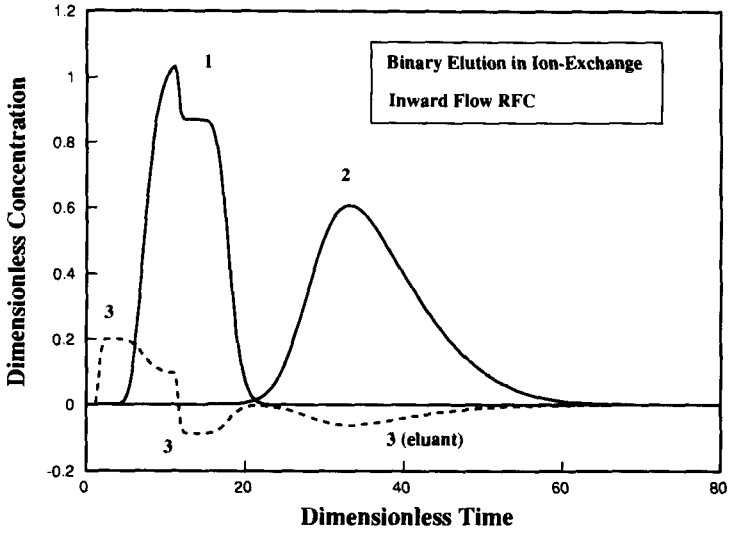

Fig. 5. Binary elution in ion-exchange RFC

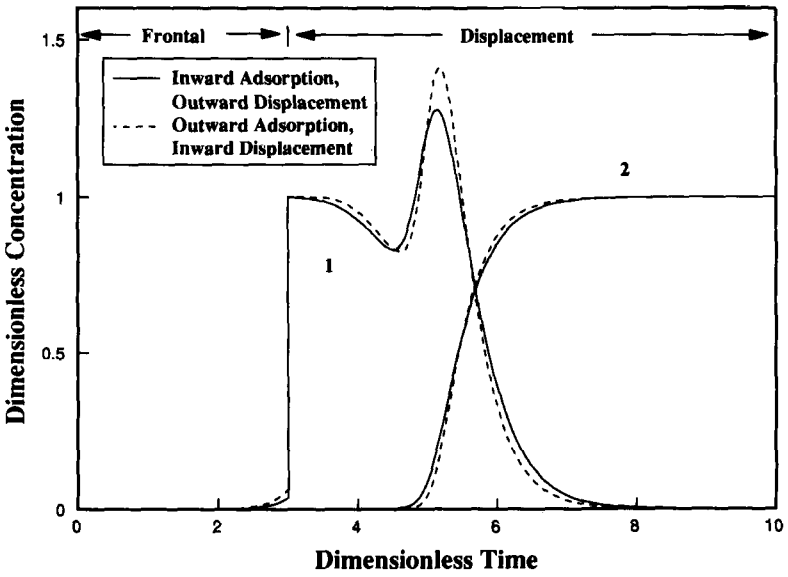

Fig. 6. Effect of RFC flow direction in reverse flow displacement

4.2 *Effect of* V_0

V_0 represents the ratio of the central cavity volume of the RFC column to the bed volume. The effect of its value on elution process is shown in Fig. 7, in which

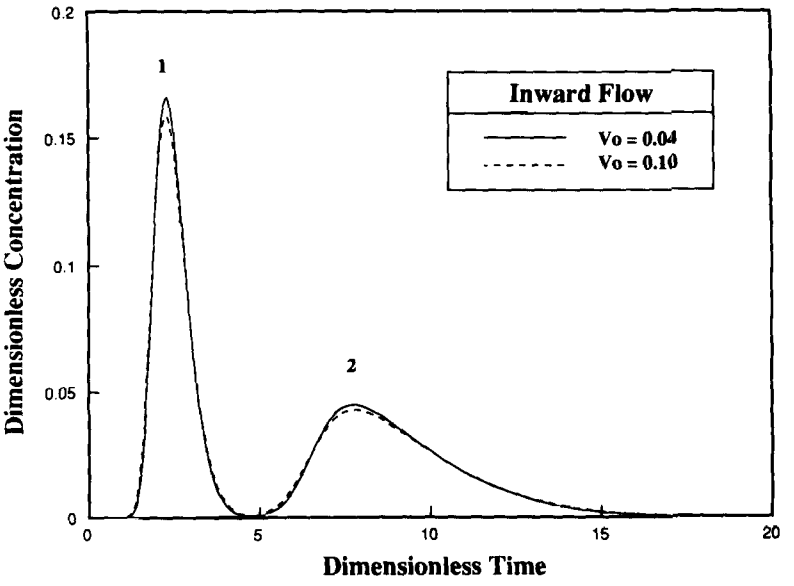

Fig. 7. Effect of V_0 on elution in inward flow RFC

the RFC column's X_1 and h are fixed while changing the X_0 value. In Fig. 7, the solid lines are the same as those in Fig. 4. The way V_0 values are changed from 0.04 to 0.1 requires that the Pe_i values for $V_0 = 0.1$ be reduced to 86.88% of those for $V_0 = 0.04$ case, and for η_i values the percentage is 94.54%. These two percentage values can easily be obtained by checking the changes in $(X_1 - X_0)$ and V_b and their relationship with Pe_i and η_i. Figure 7 shows that the peak heights are reduced and so is the peak resolution when V_0 is increased from 0.04 to 0.1. This has the same effect as reducing column length in AFC.

4.3 Effects of Pe_i, η_i and Bi_i on Elution

Figures 8 to 10 clearly show that the increase of Pe_i, η_i, or Bi_i value increases the peak heights and the peak resolution. In these three figures the solid line curves are the same as those in Fig. 4. In Fig. 8 $Pe_1 = Pe_2 = \infty$ case is plotted in order to show the errors that one may encounter if radial dispersion is neglected. In the case shown in Fig. 8 such errors are quite large. Figure 9 also indicates that the peaks are sharper if film mass transfer coefficients for the two components are larger since the dimensionless parameter η_i is proportional to k_i. Figure 11 shows that the resolution of the elution peaks is decreased if the intraparticle diffusion coefficients are reduced as reflected in the dimensionless parameters, η_i and Bi_i.

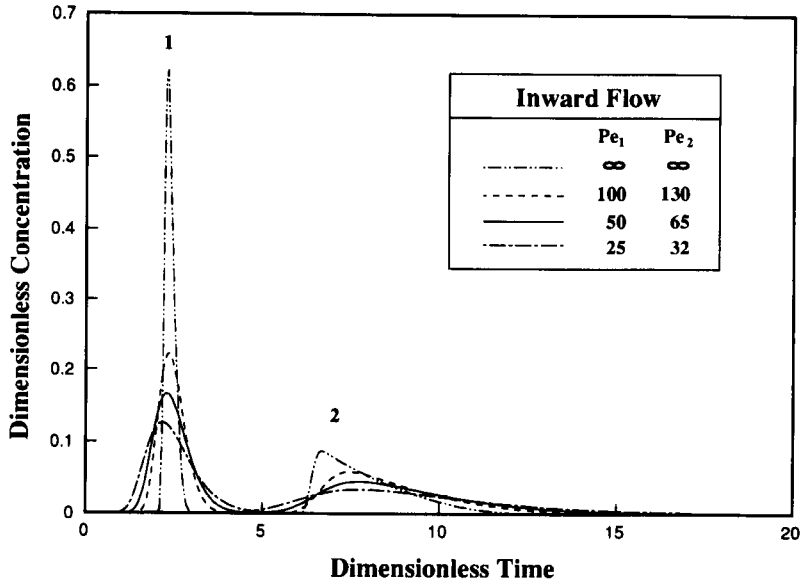

Fig. 8. Effect of Pe_i on elution in inward flow RFC

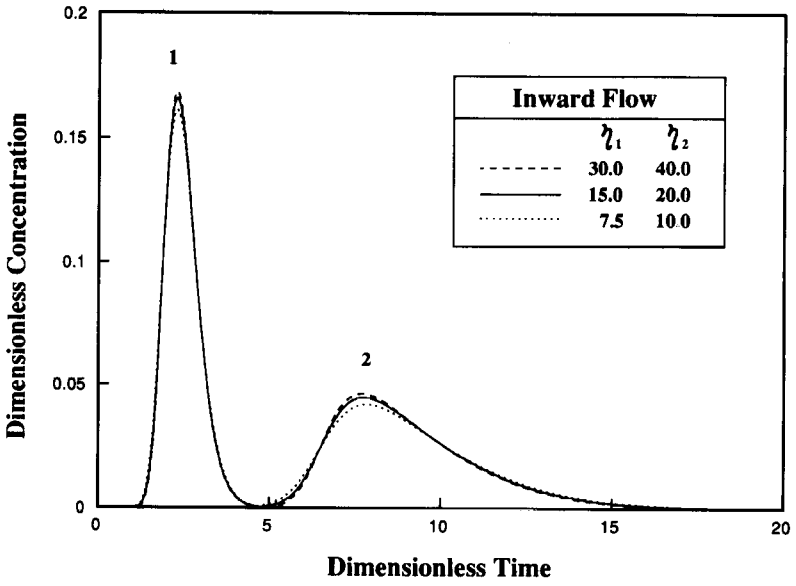

Fig. 9. Effect of η_i on elution in inward flow RFC

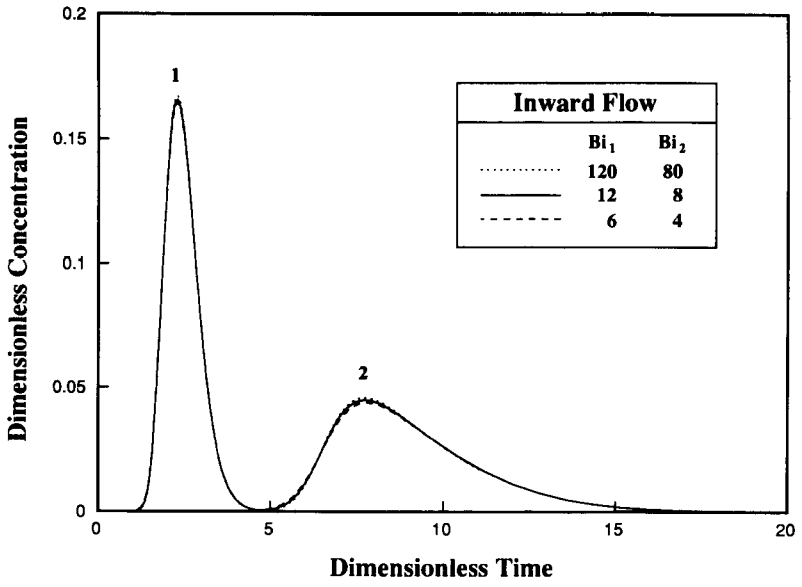

Fig. 10. Effect of Bi_i on elution in inward flow RFC

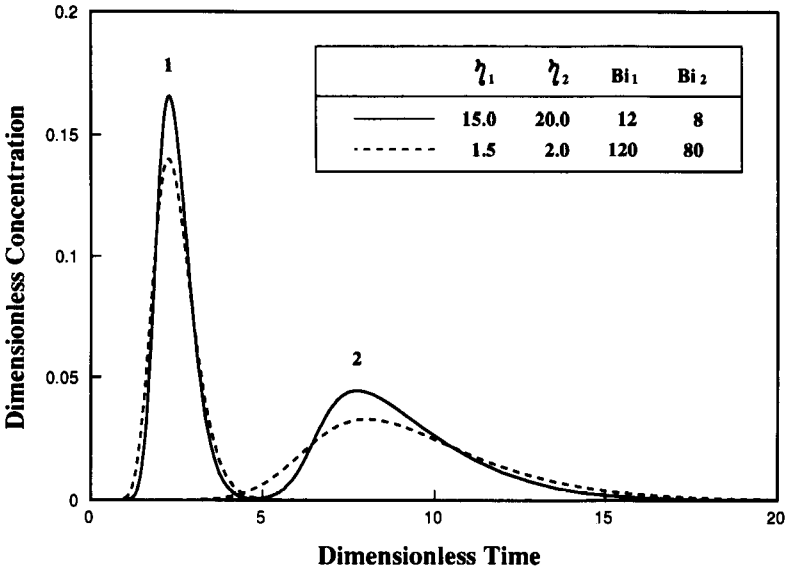

Fig. 11. Effect of D_{pi} on elution in inward flow RFC

4.4 *Effect of Treating D_{bi} and k_i as Variables*

The two component frontal adsorption system shown in Fig. 2 is chosen as a case study. Figure 12 shows three sets of inward flow breakthrough curves obtained from using the variable D_{bi} and k_i average values evaluated at V = 0.5, or $(X_1 + X_0)/2$, respectively. These three sets of curves show some differences in the sharpness and height of the "roll-up" peak. The corresponding outward flow case is given in Fig. 13. In Figs. 12 and 13, it is obvious that there are some differences among the three sets of curves in each figure caused by the way D_{bi} and k_i are treated. The average D_{bi} and ki evaluated at $(X_1 + X_0)/2$ are higher than those evaluated at V = 0.5 since $(X_1 + X_0)/2$ is closer to the center of the radial flow column than V = 0.5, and v is higher at $(X_1 + X_0)/2$. Higher D_{bi} values give lower $\overline{Pe_i}$ values and the concentration profiles tend to be more diffused, while higher k_i values give higher B_i values and the concentration profiles tend to be sharper. Between these two compromising factors, the D_{bi} *factor is more dominant than the* k_i *factor, since the dependence of* k_i *on the* coordinate X or V is much weaker.

It is well known in mass transfer studies that both Peclet and Biot numbers show some asymptotic behavior. When Pe_i values become larger, the system becomes less sensitive to the changes in Pe_i values. When Bi_i values are in the range of above 1, the higher the Bi_i values the less sensitive the system to the increase of Bi_i values. When Bi_i values are sufficiently small, the internal concentration gradient inside a particle can be neglected. On the other hand, when the Bi_i values are sufficiently large, the external interface mass transfer

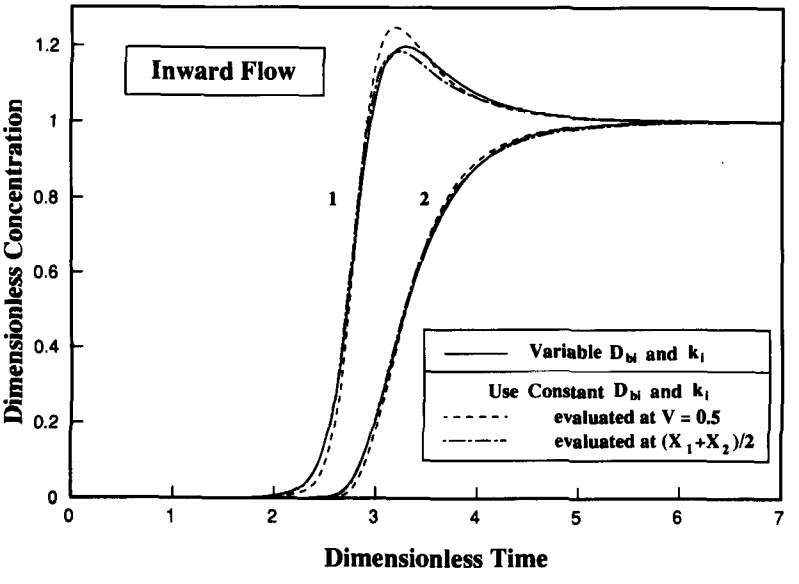

Fig. 12. Effect of treating D_{bi} and k_i as variables in inward flow RFC

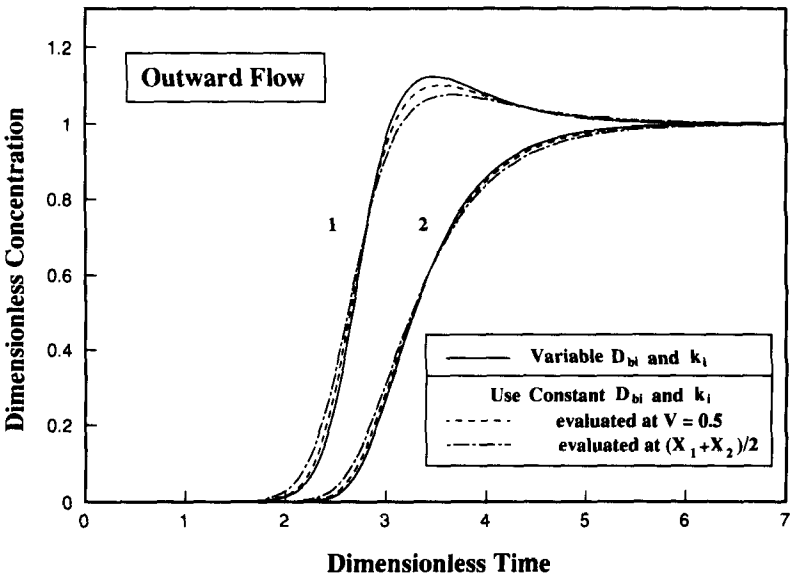

Fig. 13. Effect of treating D_{bi} and k_i as variables in outward flow RFC

resistances become negligible. These arguments are very helpful in determining the parameter ranges in which the treatment of D_{bi} and k_i as variables become important. Generally speaking, when the Pe_i values are large, the errors caused by using averaged D_{bi} valucs are small. If Bi_i values are not close to 1, then the treatment of k_i values as variables will have little effect. In most cases such averaging treatment causes some error, but they are not terribly severe. If an averaging treatment is necessary, such as in some analytical treatments in which simplification may be essential, one should not be inhibited from doing so. A good averaging method obviously can reduce error. It is difficult to provide exact general rules for averaging D_{bi} and k_i values, since the system is quite complex. From Figs. 12 and 13, and other extensive simulations, including different RFC operation and different flow directions, it is found that the averaging point should be at an X position farther away from X_0 than $(X_1 + X_0)/2$. $V = 0.5$ sometimes proves to be too close to X_1 as an averaging point, while at other times it becomes too far away, but generally speaking it is a better choice than $(X_1 + X_0)/2$. For numerical solutions it is desirable to treat D_{bi} and k_i as variable, since it is not only possible but also quite convenient if a suitable numerical procedure, such as the one presented in this chapter, is used.

4.5 Comparison of RFC and AFC

If the radial dispersion term in Eq. (9) is neglected, and ki values are treated as constants independent of the variation of v, i.e. ξ_i and Bi_i are treated as

constants, then the RFC's dimensionless PDE system, Eqs. (9) and (10), become the same as the corresponding AFC's dimensionless PDE system presented by Gu et al. [28]. Inward and outward flow difference will also disappear. This can be easily verified by using a coordinate transformation with $V^* = 1 - V$. This conclusion is, of course, valid for more simplified cases, such as the ideal RFC which neglects radial dispersion, external film mass transfer, and intra-particle diffusion. Rhee et al. [24] pointed out that system equations for ideal radial flow chromatography can be transformed to the system equations for ideal AFC with Langmuir isotherms. A similar conclusion was also reached by Rice [34] and Huang et al. [7].

The effects of radial dispersion on elution has already been shown in Fig. 9. It is often very important to account for radial dispersion in the modeling of RFC. The α values in the radial dispersion term (Eq. (9)) are in the neighborhood of 1. For $V_0 = 0.04$, one has $0.328 \leq \alpha \leq 1.672$. Comparing the definition of radial flow Peclet number in RFC with the axial flow Peclet number in AFC, it is reasonable to say that their ratio is close to $(X_1 - X_0)/L$. Obviously, Peclet numbers for radial flow in RFC are much smaller than those for axial flow in AFC. A ratio between 1:20 to 1:5 should not be uncommon. Furthermore, RFC is designed primarily for preparative and production scale separations; thus Peclet numbers for radial flow tend to be even smaller. Typical values may often be below or not very far above 100. This is in agreement with the estimation by Tharakan and Chau [17] in their study of a radial flow bio-reactor for mammalian cell culture. In preparative and large scale AFC, Peclet numbers often reach hundreds or higher and neglecting axial dispersion (i.e. assuming Peclet numbers equal to infinity) often does not give large errors. For RFC, one may not be able to make such assumptions without risking substantial errors. Thus, one should be very cautious when assuming negligible radial dispersion in RFC. In the discussion above it has been mentioned that, in RFC, radial dispersion coefficients are inversely proportional to the radial coordinate X. This is actually a very important identity of RFC arising from its special flow geometry, which also differentiates RFC from AFC in terms of dimensionless mathematical expressions. Neglecting radial dispersion in RFC means that its identity in mathematical modeling is partially lost.

As already shown in Figs. 3 to 5, if one sets the corresponding dimensionless parameters and isotherm expressions the same for both RFC and AFC, their differences in simulated effluent histories are similar. In order to have similar dimensionless constants for an AFC and an RFC, the AFC column should be a short one. Note that the dimensionless parameter V_0 is unique in RFC, and for the corresponding AFC one needs to pick the Bi_i values from the variable Bi_i values of RFC. Because of this kind of close analogy, some data obtained from a short AFC column may be used for reference in RFC. This also helps in transforming an existing AFC setup to RFC. It is also obvious that many studies for AFC, such as multicomponent interference, can be qualitatively applied to RFC.

The difference between RFC and AFC may arise from the differences in the dimensionless parameters, especially Pe_i and η_i. In reality, Pe_i and η_i values for

RFC columns are usually several times smaller than in a longer AFC column. Notice that η_i values are proportional to the "dead volume time" of the bed and this time value for RFC is often several times smaller than in AFC because of the shorter flow path in RFC. Figures 9 and 10 show that both Pe_i and η_i values are very important to the sharpness of the concentration profiles and peak resolutions. The higher the Pe_i and η_i values the better resolution. Thus, generally speaking, RFC provides lower resolution than does AFC. This is why RFC is not intended for analytical purposes. The effect arising from the difference of Bi_i values in RFC and AFC is not discussed here because of some uncertainties. Bi_i values for RFC can be either higher or lower than those in AFC depending on value ranges of v in RFC and AFC. RFC usually has a higher volumetric flow rate, but it does not necessarily have larger linear flow velocities since its cross-sectional flow area is much larger than that of AFC's.

The most important advantage of RFC over AFC with longer column is, again, that in RFC the cross-sectional area perpendicular to flow direction is very large and the flow path is relatively short. These two factors help reduce the pressure drop in the bed and permit a much higher flow rate, and thus promote productivity.

5 Extensions of the General RFC Model

All the extensions to the basic general multicomponent rate model for AFC by Gu [35] have also been applied to the RFC model. Such extensions include second order kinetics, size exclusion effect and reaction in the liquid phase for modeling of biospecific elution using soluble ligand. These extensions have been carried out with ease. Details are omitted here, since the necessary modifications for adding second order kinetics involving only the particle phase governing equation, in which the AFC and the RFC model do not differ except that the k_i values in RFC are variables. The addition of reaction terms for macromolecule and soluble ligand interaction involves the bulk-fluid phase, but it does not touch the characteristic terms of the RFC model. It has also been easily implemented [35].

6 Summary

A general nonlinear multicomponent rate model for RFC has been developed. Radial dispersion and mass transfer coefficients are treated as variables in the model. The model is solved numerically by using finite element and orthogonal collocation methods for the discretizations of bulk-fluid and particle phase PDEs, respectively. Various chromatographic operations have been simulated.

The diffusional and mass transfer effects on the RFC elution process have been studied. It has been found that for simple chromatographic operations inward flow is generally better than outward flow in RFC, since inward flow generally provides sharper concentration profiles. The treatment of radial dispersion and mass transfer coefficients by using averaged values instead of treating them as variables causes some errors and such errors may be reduced by properly taking the averages.

In numerical calculations treating the radial dispersion and mass transfer coefficients as variables adds very little complexity if the finite element method is used for the discretization of the bulk-fluid phase governing equation. It has been found that, in contrast to AFC, dispersion in the flow direction is often very important in RFC. The dynamic RFC behavior is similar to that of AFC with a shorter column, which has low Pe_i and η_i in non-dimensional analysis values. The theoretical treatment of RFC with comparison to AFC provides some useful information and it is helpful for the scale-up of RFC, either from a smaller scale RFC or from AFC to RFC. The general model has also been extended to include second order kinetics, size exclusion effect and reaction in the liquid phase for modeling of biospecific elution using soluble ligand. The numerical procedure presented in this chapter also serves as an example of how to deal with fixed bed problems involving variable physical properties.

7 References

1. McCormick D (1988) Bio/Technology 6:158
2. Saxena V, Weil AE, Kawahata RT, McGregor WC, Chandler M (1987) Am Lab (Fairfield, CT) 19:112
3. Ernst P (1987) Aust J Biotechnol 2:22
4. Chen H-L, Hou KC (1985) In: Tsao GT (ed) Annual reports on fermentation process. Academic, New York
5. Saxena V, Weil AE (1987) Bio Chromatography 2:90
6. Huang HS, Roy S, Hou C, Tsao GT (1988) Biotechnol Prog 4:159
7. Huang HS, Lee W-C, Tsao GT (1988) Chem Eng J 38:179
8. Plaigin M, Lacoste-Bourgeacq JF, Mandaro R, Lemay C (1989) Colloque INSERM 175:169
9. Lee WC, Tsai G-J, Tsao GT (1990) ACS Symp Series 427:104
10. Liapis AI (1989) J Biotech 11:143
11. Yang X, Tsai G-J, Tsao GT (1988) Third Chemical Congress of North America and 195th ACS National Meeting. Toronto
12. Balakotaiah V, Luss D (1981) AIChE J 27:442
13. Strauss A, Budde K (1978) Chem Techn 30:73
14. Hlavacek V, Votruba J (1977) In: Lapidus L, Amundson NR (eds) Chemical reactor theory: A review. Prentice-Hall, Englewood Cliffs
15. Chang H-C, Saucier M, Calo JM (1983) AIChE J 29:1039
16. Lepez de Ramos AL, Pironti FF (1987) AIChE J 33:1747
17. Tharakan J, Chau PC (1987) Biotechnol Bioeng 29:657
18. Lapidus L, Amundson NR (1950) J Phys Colloid Chem 54:821
19. Rachinskii VV (1968) J Chromatogr 33:234
20. Inchin PA, Rachinskii VV (1977) Russ J Phys Chem 47:1331
21. Lee W-C, Huang SH, Tsao GT (1988) AIChE J 34:2083

22. Kalinichev AI, Zolotarev PP (1977) Russ J Phys Chem 51:871
23. Lee WC (1989) PhD Thesis, Purdue University, West Lafayette
24. Rhee H-K, Aris R, Amundson NR (1970) Philos Trans R Soc (London) Ser A 267:419
25. Helfferich F (1962) J. Am Chem Soc 84:3242
26. Slattery JC (1981) Momentum, energy and mass transfer in continua. McGraw-Hill, New York
27. Gu T, Tsai G-J, Tsao GT (1991) Chem Eng Sci 46:1279
28. Gu T, Tsai G-J, Tsao GT (1990) AIChE J 36:781
29. Finlayson BA (1980) Nonlinear analysis in chemical engineering. McGraw-Hill, New York
30. Reddy JN (1984) An introduction to the finite element method. McGraw Hill, New York
31. Weber SG, Carr PW (1989) In: Brown PR, Hartwick RA (eds) High performance liquid chromatography. Wiley, New York
32. Ruthven DM (1984) Principles of adsorption and adsorption processes. Wiley, New York
33. Chase HA (1985) In: Vedrrall MS (ed) Discovery and isolation of microbial products. Ellis Horwood, Chichester
34. Rice RG (1982) Chem Eng Sci 37:83
35. Gu T (1990) PhD Thesis, Purdue University, West Lafayette